

## **FIREcaller: Detecting Frequently Interacting Regions from Hi-C Data**

Cheyenna Crowley<sup>1,2</sup>, Yuchen Yang<sup>1</sup>, Yunjiang Qiu<sup>3,4</sup>, Benxia Hu<sup>1,5</sup>, Jakub Lipiński<sup>6</sup>, Dariusz Plewczynski<sup>6,7</sup>, Hyejung Won<sup>1,5</sup>, Bing Ren<sup>3,8,9</sup>, Ming Hu<sup>10+</sup>, Yun Li<sup>1,2,11+</sup>

<sup>1</sup> Department of Genetics, University of North Carolina Chapel Hill, Chapel Hill, NC , USA.

<sup>2</sup> Department of Biostatistics, University of North Carolina Chapel Hill, Chapel Hill, NC , USA.

<sup>3</sup> Ludwig Institute for Cancer Research, La Jolla, California, USA.

<sup>4</sup> Bioinformatics and Systems Biology Graduate Program, University of California San Diego, La Jolla, California, USA

<sup>5</sup> UNC Neuroscience Center, University of North Carolina Chapel Hill, Chapel Hill, NC , USA.

<sup>6</sup> Cellular Genomics, Warsaw, Poland.

<sup>7</sup> Department of Mathematics and Information Science, Warsaw University of Technology, Warszawa, Poland.

<sup>8</sup> Department of Cellular and Molecular Medicine, University of California San Diego. La Jolla, California USA.

<sup>9</sup> Institute of Genomic Medicine and Moores Cancer Center, University of California San Diego. La Jolla, California, USA.

<sup>10</sup> Department of Quantitative Health Sciences, Lerner Research Institute, Cleveland Clinic Foundation, Cleveland, Ohio, USA.

<sup>11</sup> Department of Computer Science University of North Carolina Chapel Hill, Chapel Hill, NC , USA.

+ Indicates Corresponding Author

### **Abstract:**

Hi-C experiments have been widely adopted to study chromatin spatial organization, which plays an essential role in genome function. We have recently identified frequently interacting regions (FIREs) and found that they are closely associated with cell type-specific gene regulation. However, computational tools for detecting FIREs from Hi-C data are still lacking. In this work, we present FIREcaller, a stand-alone, user-friendly R package for detecting FIREs from Hi-C data. FIREcaller takes raw Hi-C contact matrices as input, performs within-sample and cross-sample normalization, and outputs continuous FIRE scores, dichotomous FIREs, and super-FIREs. Applying FIREcaller to Hi-C data from various human tissues, we demonstrate that FIREs and superFIREs identified, in a tissue specific manner, are closely related to transcription regulation, are enriched in enhancer-promoter (E-P) interactions, tend to co-localize with regions exhibiting epigenomic signatures of regulatory roles, and aid the interpretation of prioritization of GWAS variants. The FIREcaller package is implemented in R and freely available at <https://yunliweb.its.unc.edu/FIREcaller>.

### **Highlights:**

- Frequently Interacting Regions (FIREs) can be used to identify tissue and cell type-specific regulatory regions.
- An R software, FIREcaller, has been developed to identify FIREs and clustered FIREs called super-FIREs.

## **1. Introduction**

Chromatin folding in the three-dimensional (3D) space is closely related to genome function [1]. In particular, transcription regulation is orchestrated by a collection of *cis*-regulatory elements,

including promoters, enhancers, insulators, and silencers. Alteration of chromatin spatial organization in the human genome can lead to gene dysregulation and consequently, complex diseases including developmental disorders and cancers [2, 3].

High-throughput chromatin conformation capture (Hi-C) has been widely used to measure genome-wide chromatin spatial organization since first introduced in 2009 [4-6]. Analyzing Hi-C data has led to the discovery of structural readouts at a cascade of resolutions, including A/B compartments [6], topologically associating domains (TADs) [7], chromatin loops [8], and statistically significant long-range chromatin interactions [9-11]. Among these Hi-C readouts, TADs and chromatin loops are largely conserved across cell types [12, 13], while A/B compartments and long-range chromatin interactions exhibit rather moderate levels of cell type specificity [6, 7].

As an attempt to identify Hi-C readouts that are better indicative of cell type or tissue-specific chromatin spatial organizations, we have in our previous work [14], identified thousands of frequently interacting regions (FIREs) by studying a compendium of Hi-C datasets across 14 human primary tissues and 7 cell types. We defined FIREs as genomic regions with significantly higher local chromatin interactions than expected under the null hypothesis of random collisions [14].

FIREs are distinct from previously discovered Hi-C structural readouts such as A/B compartments, TADs, and chromatin loops. In general, FIREs tend to reside at the center of TADs, associate with intra-TAD E-P interactions, and are contained within broader regions of active chromatin [14]. FIREs are tissue and cell type-specific, and enriched for tissue-specific enhancers and nearby tissue-specifically expressed genes, suggesting their potential relevance to tissue-specific transcription regulatory programs. FIREs are also conserved between human and mouse. In addition, FIREs have been revealed to occur near cell-identity genes and active enhancers [14]. Thus, FIREs have proven valuable in identifying tissue and cell type-specific regulatory regions, functionally conserved regions such as enhancers shared by human and mouse, and in interpreting genetic variants associated with human complex diseases and traits [14-16].

Since the discovery of FIREs, we have collaborated with multiple groups to further demonstrate their values in various applications, resulting in multiple recent preprints and publications [16-19]. For example, in an analysis of adult and fetal cortex Hi-C datasets, FIREs and super-FIREs recapitulated key functions of tissue specificity, such as neurogenesis in fetal cortex and core neuronal functions in adult cortex [19]. In addition, evolutionary analyses revealed that these brain FIRE regions have stronger evidence for ancient and recent positive selection, less population differentiation, and fewer rare genetic variants [19]. For another example, Gorkin et al. [16] investigated how 3D chromatin conformation in lymphoblastoid cell lines (LCL) varies across 20 individuals. They reported that FIREs are significantly enriched in LCL-specific enhancers, super-

enhancers, and immune related biological pathways and disease ontologies, further demonstrating the close relationship between FIREs and *cis*-regulatory elements [16]. In particular, even with the sample size of  $\leq 20$  individuals, hundreds of FIRE-QTLs (that is, genetic variants associated with the strength of FIRE) have been reported, suggesting that FIREs show strong evidence of genetic regulation.

Despite the importance and utilities of FIREs, only in-house pipelines exist for detecting FIREs, limiting the general application of FIRE analysis and the full exploration of cell type-specific chromatin spatial organization features from Hi-C data. In this work, we developed FIREcaller, a stand-alone, user-friendly R package for detecting FIREs from Hi-C data as an implementation of the method described in our previous work [14].

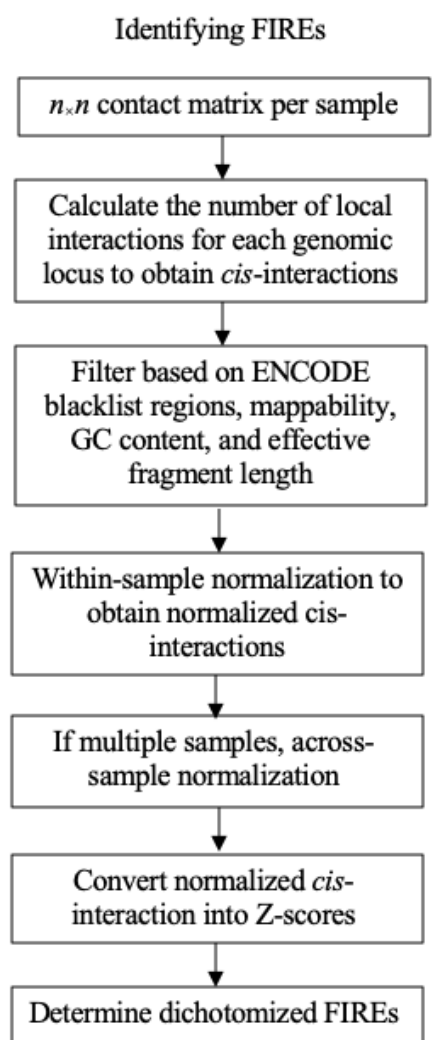


**Figure 1. Flow Chart of calling FIREs using the FIREcaller Software**

## 2. Materials and Methods

### 2.1 Input Matrix

First, FIREcaller takes an  $n \times n$  Hi-C contact matrix as input. The contact matrix  $M$  is constructed by dividing the genome into bins of size  $b$  consecutive non-overlapping regions for each chromosome. In our original work [14],  $b$  was fixed at 40Kb. In this FIREcaller work, we allow  $b$  to be 10Kb, 20Kb, or the default 40Kb. Each entry in the contact matrix  $M$ ,  $m_{ij}$ , corresponds to the number of reads mapped between locus/bin  $i$  and locus/bin  $j$ . The corresponding symmetric  $n \times n$  matrix reflects the number of mapped intra-chromosomal reads between each pair of loci [6]. We removed all intra-chromosomal contacts within 15Kb to filter out reads due to self-ligation.

Recommendations for the resolution of the input matrix depend on the sequencing depth of the input Hi-C data. Specifically, we recommend using a 10Kb bin resolution for Hi-C data with  $\sim 2$  billion reads, and a 40Kb bin resolution for Hi-C data with  $\sim 500$  million reads [6, 8, 20-23] (**Supplement Information S1**).

### 2.2 Cis-Interaction Calculation

Taking the  $n \times n$  contact matrix as input, FIREcaller calculates the total number of local *cis*-interactions for each genomic locus (40Kb bin size by default). Following our previous work [14], we define local to be within  $\sim 200$ Kb by default. This threshold is largely driven by empirical

evidences showing that contact domains exert influences on transcription regulation within 200Kb. For instance, contact domains reported in human GM12878 from *in-situ* Hi-C are at a median size of 185 kb [8, 20]. In addition, Jin et al. reported a median distance of E-P interactions at 124Kb [21], Song et al. reported 80% of promoter interacting regions within 160Kb [24], and Jung et al. found promoter centered long-range chromatin interactions with median distance 158 Kb [25]. Consistently, an analysis of the dorsolateral prefrontal cortex sample [26] showed E-P interactions at a median distance of 157Kb, and our study showed adult cortex E-P interactions at a median distance of 190Kb [19] (**Supplement Information S2**). On the other hand, multiple *cis*-regulatory regions have been shown to control their target genes from longer genomic distances [3, 19, 20, 27]. To accommodate these longer-range chromatin interactions our FIREcaller package allows a user-specified upper bound of the *cis*-interacting regions.

### 2.3 Bin level filtering

Bins are then filtered based on multiple criteria that may lead to systematic biases, including effective restriction fragment lengths which measures the density of the restriction enzyme cut sites within each bin, GC content, and sequence uniqueness [28, 29]. FIREcaller removes bins with 0 mappability, 0 GC content or 0 effective fragment length. We also remove bins for which more than 25% of their neighborhood (within 200Kb, by default) bins have 0 mappability, 0 GC content or 0 effective fragment length. Finally, any bins overlapped within the MHC region or the ENCODE blacklist regions [30] are also filtered out.

### 2.4 Within-sample Normalization

FIREcaller then uses the HiCNormCis method [14] to conduct within-sample normalization. HiCNormCis adopts a Poisson regression approach, adjusting for the three major sources of systematic biases: effective fragment length determined by restriction enzyme cutting frequency, GC content, and mappability [14].

Let  $U_i$ ,  $F_i$ ,  $GC_i$  and  $M_i$  represent the total *cis*-interactions (15-200Kb, by default), effective fragment length, GC content, and mappability for bin  $i$ , respectively. We assume that  $U_i$  follows a Poisson distribution, with mean  $\theta_i$ , where  $\log(\theta_i) = \beta_0 + \beta_F F_i + \beta_{GC} GC_i + \beta_M M_i$ . After fitting the Poisson regression model, we define the residuals  $R_i$  as the normalized *cis*-interaction for bin  $i$ .

FIREcaller fits a Poisson regression model by default. Users can also fit a negative binomial regression model. In practice, both Poisson regression and negative binomial regression model achieved similar effect of bias removal, while Poisson regression is computationally more efficient (**Supplement Information S3**).

## 2.5 Across-sample Normalization

If the user provided multiple Hi-C datasets, FIREcaller uses the R function “*normalize.quantiles*” in the “*preprocessCore*” package to perform quantile normalization of the normalized *cis*-interactions across samples [31].

## 2.6 Identifying Significant Frequently Interacting Regions

FIREcaller then converts the normalized *cis*-interactions into Z-scores, calculates one-sided *p*-values based on the standard normal distribution, and classifies bins with *p*-value < 0.05 as FIREs. The output file contains, for each bin, the normalized *cis*-interactions, the  $-\ln(p\text{-value})$  (i.e., the continuous FIREscore), and the dichotomized FIRE or non-FIRE classification.

## 2.7 Detecting Super-FIREs

FIREcaller also identifies clustered FIREs, termed as super-FIRE (**Figure 2**). We first concatenate all consecutive FIRE bins, and sum their continuous FIREscores. We then plot the summed continuous FIREscores for the clustered FIREs against their ranks to identify the inflection point where the slope of the tangent line is one. Super-FIREs are defined as all clustered FIREs on the right of the inflection point [14, 19]. This method is adapted from the Ranking of Super Enhancer (ROSE) algorithm [32], which was originally proposed for the identification of super-enhancers.

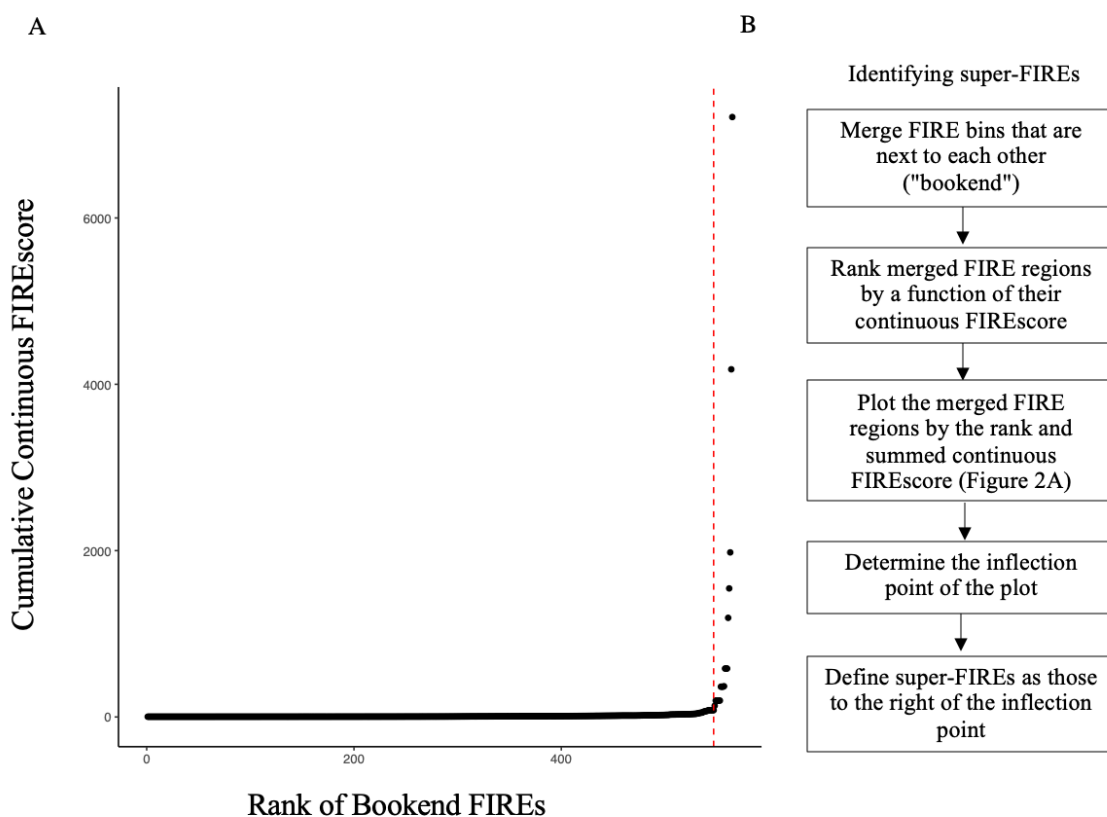


**Figure 2. Flow chart for identifying super-FIREs.** A) Scatterplot of clustered FIREs ranked by their continuous FIREscores, ordered from least interactive (left) to most interactive (right). Red dashed line highlights the inflection point of the curve. B) Flow chart for super-FIRE identification.

### 3. Results

#### 3.1 An Illustrative Example

We used the Hi-C data from human hippocampus tissue in our previous study [14] to showcase the utility of FIREcaller. **Figure 3** shows an illustrative example of a 400Kb super-FIRE (merged from 10 consecutive bins, and marked by the red horizontal bar in the “FIREs” track), which overlaps with two hippocampus super-enhancers (indicated by the two light blue horizontal bars in the “Enhancers” track). Notably, this super-FIRE contains a schizophrenia-associated GWAS SNP rs9960767 (black vertical line) [33], and largely overlaps with gene *TCF4* (chr18: 52,889,562-53,332,018; pink horizontal bar depicted at the top), which plays an important role in neurodevelopment [34]. Since rs9960767 resides within a super-FIRE with highly frequent local chromatin interactions, we hypothesize that chromatin spatial organization may play an important role in gene regulation in this region, elucidating potential mechanism by which rs9960767 affects schizophrenia risk.

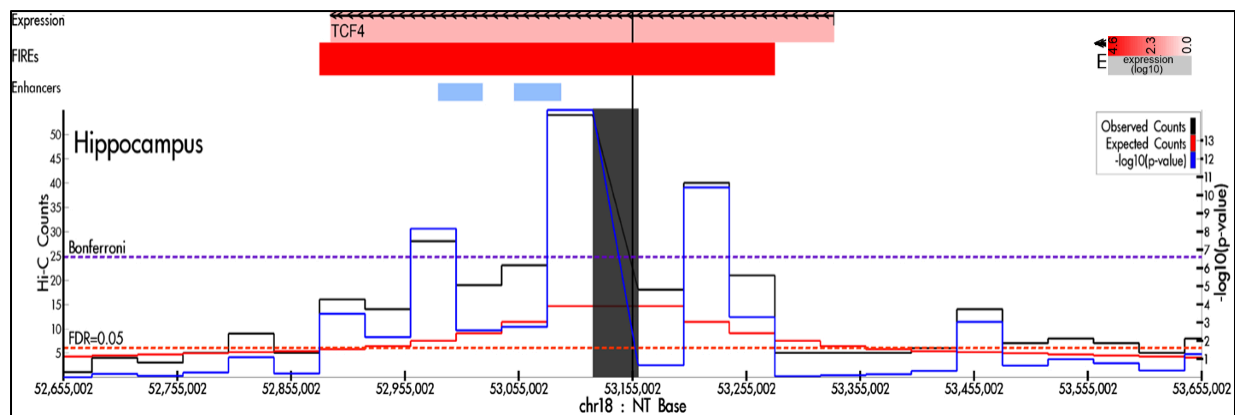


**Figure 3. An example of a super-FIRE in human hippocampus tissue.** Virtual 4C plot of a 1Mb region (chr18:52,665,002-53,665,002) anchored at the schizophrenia-associated GWAS SNP rs9960767 (black vertical line), visualized by HUGIn [35]. The solid black, red and blue lines represent the observed contact frequency, expected contact frequency, and  $-\log_{10}(p\text{-value})$  from Fit-Hi-C [36], respectively. The dashed purple and red lines represent significant thresholds corresponding to Bonferroni correction and 5% FDR, respectively. The red horizontal bar in the “FIREs” track depicts the 400Kb super-FIRE region. The two blue horizontal bars in the “Enhancers” track mark the two hippocampus super-enhancers in the region.

#### 3.2 Integrative Analysis of FIREs with Gene Expression in Human Brain Tissue

To investigate the relationship between FIREs and tissue-specifically expressed genes, we applied FIREcaller to Hi-C data from fetal [37] and adult [38] cortical tissues, and identified 3,925 fetal FIREs and 3,926 adult FIREs. Among them, 2,407 FIREs are fetal-specific and 2,408 FIREs are

adult-specific (the remaining 1,518 FIREs are shared). We observed massive changes in FIREs between fetal and adult which recapitulate recently reported extensive chromatin rewiring during brain development [38], exemplifying the cell type-specific nature of FIREs. We then overlapped FIREs with gene promoters and found that the dynamics of FIREs across brain developmental stages are closely associated with gene regulation dynamics during brain development (**Figure 4**). Specifically, we examined expression levels of genes whose promoters (defined as  $\pm 500$  bp of transcription start site [TSS]) overlap with fetal brain-specific FIREs and are expressed in fetal brain, similarly genes whose promoter overlap with adult brain-specific FIREs and are expressed in adult brain. Gene expression data in both fetal and adult brain cortex are from two of our recent studies [37, 38]. These criteria resulted in 707 and 882 genes in fetal and adult brain, respectively. Among them, 412 are fetal brain specific, 587 are adult brain specific, and 295 genes are shared (**Table 1**).

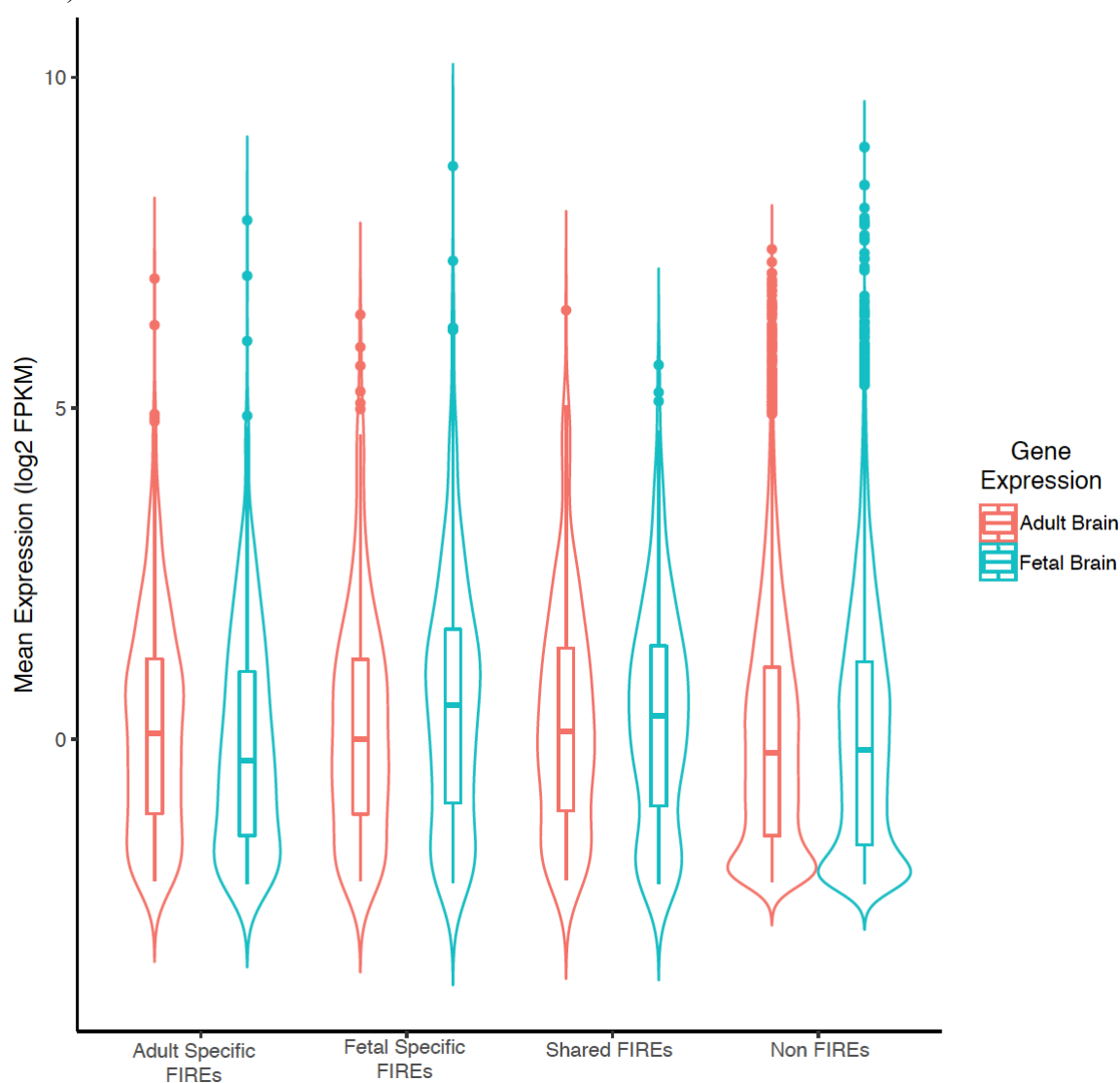


**Figure 4. Distribution of expression for genes overlapping fetal or adult brain FIREs.** The leftmost pair of violin boxplots shows the expression profile of the 587 genes mapped to adult brain-specific FIREs, with expression measured in fetal brain cortex (blue) and adult brain cortex (red), respectively. The second pair of violin boxplots shows the expression profile of the 412 genes mapped to fetal brain-specific FIREs, again in fetal brain cortex (blue) and adult brain cortex (red), respectively. The third pair shows the expression profile of the 295 genes mapped to FIREs shared between fetal and adult brain, yet again in fetal brain cortex (blue) and in adult brain cortex (red). The pair to the farthest right, shows the expression profile of genes not overlapping any FIREs, with a total of 15640 such genes (labelled “Non FIREs”).

	# FIREs	# FIREs overlapping with a gene	#of genes overlapping FIREs
Adult-specific	2,408	488	587
Fetal-specific	2,407	338	412
Shared	1,518	258	295

**Table 1. Tissue-Specific FIREs and Shared FIREs, and Overlapping Genes.**

For the 587 genes mapped to adult brain-specific FIREs, the mean gene expression levels, measured by  $\log_2(\text{FPKM})$ , are  $-0.052$  and  $0.190$  in fetal and adult brain cortex, respectively. These 587 genes are significantly up-regulated in adult brain ( $p\text{-value} = 1.3 \times 10^{-10}$  **Figure 4; Table S3**). Meanwhile, for the 412 genes mapped to fetal brain-specific FIREs, the mean gene expression levels, again measured by  $\log_2(\text{FPKM})$ , are  $0.551$  and  $0.209$  in fetal and adult brain cortex, respectively. These 412 genes are significantly up-regulated in fetal brain (paired t-test  $p\text{-value} = 7.8 \times 10^{-13}$ ) (**Figure 4; Table S3**). By contrast, for the 295 genes co-localizing with FIREs shared between fetal and adult cortex, the mean gene expression levels are  $0.328$  and  $0.312$  in fetal and adult brain cortex, respectively. These 295 genes show no significant difference in their expression levels in adult and fetal brain ( $p\text{-value} = 0.79$ ). Similarly and finally, genes not overlapping any FIREs exhibit no significant expression differences in fetal and adult brains either ( $p\text{-value} = 0.96$ ) (**Figure 4**).

### 3.3 Integrative Analysis of FIREs and Enhancer-Promoter Interactions

We used Hi-C data from left ventricle and liver tissues from Schmitt et al study [14], and applied Fit-Hi-C [39] to call significant chromatin interactions at 40Kb bin resolution. We only considered bin pairs within 2Mb distance. Next, we used H3K27ac ChIP-seq peaks [40] in left ventricle and liver tissue to define active enhancers, and used 500 bp upstream / downstream of TSS to define promoters. A pair of 40Kb bins is defined as an E-P interaction if one bin contains a promoter, and the other bin contains an active enhancer. In total, at an FDR of 1%, we identified 41,401 and 30,569 E-P interactions in left ventricle and liver, respectively. Among them, 29,096 are left ventricle-specific, and 18,264 liver-specific.

At the same 40Kb bin resolution, applying our FIREcaller, we identified 3,643 FIREs in left ventricle and 3,642 FIREs in liver, with 1,186 shared between these two tissues. We found that



FIREs are enriched for E-P interactions compared to non-FIREs for both liver and left ventricle (liver: odds ratio [OR] = 7.2, Fisher's exact test p-value <  $2.2 \times 10^{-16}$ ; left ventricle: OR = 4.0, p-value <  $2.2 \times 10^{-16}$ ). Comparing between two tissues, we observed that left ventricle-specific E-P interactions are highly enriched in left ventricle-specific FIREs and liver specific E-P interactions highly enriched in liver specific FIREs (OR=3.8, p-value <  $2.2 \times 10^{-16}$ ; **Table 2**). Our results demonstrate that the tissue-specificity of FIREs is closely associated with the tissue-specificity of E-P interactions [14].

	Left Ventricle Specific E-P	Liver Specific E-P
Left Ventricle- Specific FIRE	1,093	416
Liver-Specific FIRE	951	1,392

**Table 2. Tissue-Specific FIREs and Tissue Specific E-P interactions in Liver and Left Ventricle tissues.** In the table, we count the numbers of tissue specific E-P interactions involving tissue specific FIREs. For example, 1,093 means there are 1,093 left ventricle specific E-P interactions involving left ventricle specific FIREs. Similarly for the remaining three counts.

### 3.4 Integrative Analysis of FIREs and ChIP-seq Peaks.

Next, we evaluated the relationship between FIREs and histone modifications in cortex [26, 38, 40]. We found that H3K4me3 and H3K27ac ChIP-seq peaks are both enriched at FIRE regions (**Figure 5**).

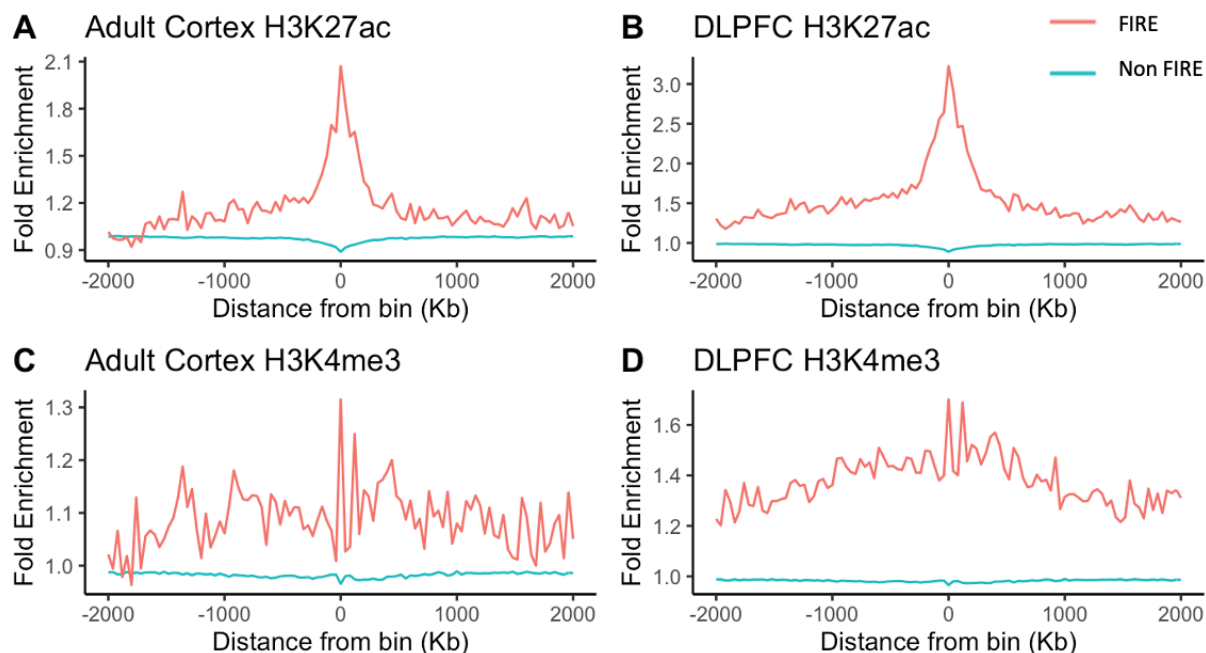


**Figure 5. H3K4me3 and H3K27ac ChIP-seq peaks are enriched at FIREs.** X axis is the distance from a bin, with the bins grouped into FIRE bins and non FIRE bins. Y axis is fold enrichment quantified by MACS[41] when applied to the corresponding histone ChIP-seq data.

## 4. Conclusion

In this paper, we present FIREcaller, a user-friendly R package to identify FIREs from Hi-C data. We demonstrate its utilities through applications to multiple Hi-C datasets and integrative analyses with E-P interactions, histone modifications and gene expression. We believe that FIREcaller will become a useful tool in studying cell type or tissue specific chromatin spatial organization.

## 5. Funding

This research was supported by the National Institute of Health grants R01HL129132 and P50HD103573 (awarded to YL), U54DK107977 (awarded to BR and MH), and R00-MH113823 (awarded to HW). YL is also partially supported by R01GM105785. *Conflict of interest*: none declared.

## 6. Authors' Contributions

**Cheyanna Crowley**: Software, Validation, Formal Analysis, Writing – Original Draft. **Yuchen Yang**: Validation, Formal Analysis. **Yunjiang Qiu**: Methodology, Resources. **Benxia Hu**: Formal Analysis, Resources. **Jakub Lipiński**: Resources. **Dariusz Plewczyński**: Resources. **Hyejung Won**: Formal Analysis, Resources, Funding Acquisition. **Bing Ren**: Methodology, Funding Acquisition. **Ming Hu**: Supervision, Methodology, Writing- Review & Editing, Funding Acquisition. **Yun Li**: Supervision, Validation, Writing- Review & Editing, Funding Acquisition.

## 7. References

1. Dekker, J., M.A. Marti-Renom, and L.A. Mirny, *Exploring the three-dimensional organization of genomes: interpreting chromatin interaction data*. Nat Rev Genet, 2013. **14**(6): p. 390-403.
2. Krijger, P.H. and W. de Laat, *Regulation of disease-associated gene expression in the 3D genome*. Nat Rev Mol Cell Biol, 2016. **17**(12): p. 771-782.
3. Li, Y., M. Hu, and Y. Shen, *Gene regulation in the 3D genome*. Hum Mol Genet, 2018. **27**(R2): p. R228-R233.
4. Tjong, H., et al., *Population-based 3D genome structure analysis reveals driving forces in spatial genome organization*. Proc Natl Acad Sci U S A, 2016. **113**(12): p. E1663-72.
5. Yardimci, G.G., et al., *Measuring the reproducibility and quality of Hi-C data*. Genome Biol, 2019. **20**(1): p. 57.
6. Lieberman-Aiden, E., et al., *Comprehensive Mapping of Long-Range Interactions Reveals Folding Principles of the Human Genome*. Science, 2009. **326**(5950): p. 289.
7. Dixon, J.R., D.U. Gorkin, and B. Ren, *Chromatin Domains: the Unit of Chromosome Organization*. Molecular cell, 2016. **62**(5): p. 668-680.
8. Rao, S.S.P., et al., *A three-dimensional map of the human genome at kilobase resolution reveals principles of chromatin looping*. Cell, 2014. **159**(7): p. 1665-1680.
9. Kaul, A., S. Bhattacharyya, and F. Ay, *Identifying statistically significant chromatin contacts from Hi-C data with FitHiC2*. Nat Protoc, 2020. **15**(3): p. 991-1012.
10. Xu, Z., et al., *A hidden Markov random field-based Bayesian method for the detection of long-range chromosomal interactions in Hi-C data*. Bioinformatics, 2016. **32**(5): p. 650-6.
11. Xu, Z., et al., *FastHiC: a fast and accurate algorithm to detect long-range chromosomal interactions from Hi-C data*. Bioinformatics, 2016. **32**(17): p. 2692-5.
12. Dixon, J.R., et al., *Topological Domains in Mammalian Genomes Identified by Analysis of Chromatin Interactions*. Nature, 2012. **485**(7398): p. 376-380.
13. Rao, Suhas S.P., et al., *A 3D Map of the Human Genome at Kilobase Resolution Reveals Principles of Chromatin Looping*. Cell, 2014. **159**(7): p. 1665-1680.
14. Schmitt, A.D., et al., *A Compendium of Chromatin Contact Maps Reveal Spatially Active Regions in the Human Genome*. Cell reports, 2016. **17**(8): p. 2042-2059.

15. Burgess, D.J., *Epigenomics: Deciphering non-coding variation with 3D epigenomics*. Nat Rev Genet, 2016. **18**(1): p. 4.
16. Gorkin, D.U., et al., *Common DNA sequence variation influences 3-dimensional conformation of the human genome*. Genome Biol, 2019. **20**(1): p. 255.
17. Hu, B., et al., *Neuronal and glial 3D chromatin architecture illustrates cellular etiology of brain disorders*. bioRxiv, 2020: p. 2020.05.14.096917.
18. Halvorsen, M., et al., *Increased burden of ultra-rare structural variants localizing to boundaries of topologically associated domains in schizophrenia*. Nat Commun, 2020. **11**(1): p. 1842.
19. Giusti-Rodríguez, P., et al., *Using three-dimensional regulatory chromatin interactions from adult and fetal cortex to interpret genetic results for psychiatric disorders and cognitive traits*. bioRxiv, 2019: p. 406330.
20. Yu, M. and B. Ren, *The Three-Dimensional Organization of Mammalian Genomes*. Annu Rev Cell Dev Biol, 2017. **33**: p. 265-289.
21. Jin, F., et al., *A high-resolution map of three-dimensional chromatin interactome in human cells*. Nature, 2013. **503**(7475): p. 290-294.
22. Schmitt, A.D., M. Hu, and B. Ren, *Genome-wide mapping and analysis of chromosome architecture*. Nature Reviews Molecular Cell Biology, 2016. **17**: p. 743.
23. Lajoie, B.R., J. Dekker, and N. Kaplan, *The Hitchhiker's Guide to Hi-C Analysis: Practical guidelines*. Methods (San Diego, Calif.), 2015. **72**: p. 65-75.
24. Song, M., et al., *Mapping cis-regulatory chromatin contacts in neural cells links neuropsychiatric disorder risk variants to target genes*. Nat Genet, 2019. **51**(8): p. 1252-1262.
25. Jung, I., et al., *A compendium of promoter-centered long-range chromatin interactions in the human genome*. Nat Genet, 2019. **51**(10): p. 1442-1449.
26. Li, M., et al., *Integrative functional genomic analysis of human brain development and neuropsychiatric risks*. Science, 2018. **362**(6420): p. eaat7615.
27. Fulco, C.P., et al., *Systematic mapping of functional enhancer-promoter connections with CRISPR interference*. Science, 2016. **354**(6313): p. 769-773.
28. Hu, M., et al., *HiCNorm: removing biases in Hi-C data via Poisson regression*. Bioinformatics, 2012. **28**(23): p. 3131-3133.
29. Yaffe, E. and A. Tanay, *Probabilistic modeling of Hi-C contact maps eliminates systematic biases to characterize global chromosomal architecture*. Nat Genet, 2011. **43**(11): p. 1059-65.
30. Amemiya, H.M., A. Kundaje, and A.P. Boyle, *The ENCODE Blacklist: Identification of Problematic Regions of the Genome*. Scientific Reports, 2019. **9**(1): p. 9354.
31. Bolstad, B.M., et al., *A comparison of normalization methods for high density oligonucleotide array data based on variance and bias*. Bioinformatics, 2003. **19**(2): p. 185-93.
32. Whyte, W.A., et al., *Master transcription factors and mediator establish super-enhancers at key cell identity genes*. Cell, 2013. **153**(2): p. 307-319.
33. Stefansson, H., et al., *Common variants conferring risk of schizophrenia*. Nature, 2009. **460**(7256): p. 744-7.
34. Forrest, M.P., et al., *The emerging roles of TCF4 in disease and development*. Trends Mol Med, 2014. **20**(6): p. 322-31.
35. Martin, J.S., et al., *HUGIn: Hi-C Unifying Genomic Interrogator*. Bioinformatics, 2017.
36. Ay, F., T.L. Bailey, and W.S. Noble, *Statistical confidence estimation for Hi-C data reveals regulatory chromatin contacts*. Genome Res, 2014.
37. Won, H., et al., *Chromosome conformation elucidates regulatory relationships in developing human brain*. Nature, 2016. **538**(7626): p. 523-527.
38. Wang, D., et al., *Comprehensive functional genomic resource and integrative model for the human brain*. Science (New York, N.Y.), 2018. **362**(6420): p. eaat8464.
39. Ay, F., T.L. Bailey, and W.S. Noble, *Statistical confidence estimation for Hi-C data reveals regulatory chromatin contacts*. Genome research, 2014. **24**(6): p. 999-1011.
40. Kundaje, A., et al., *Integrative analysis of 111 reference human epigenomes*. Nature, 2015. **518**(7539): p. 317-330.
41. Zhang, Y., et al., *Model-based analysis of ChIP-Seq (MACS)*. Genome Biol, 2008. **9**(9): p. R137.